

1                                   **Coupling Mars ground and orbital views:**  
2                                   **generate viewsheds of Mastcam images from the Curiosity rover,**  
3                                   **using ArcGIS® and public datasets.**  
4

5 Authors: M. Nachon<sup>1</sup>, S. Borges<sup>2</sup>, R.C. Ewing<sup>1</sup>, F. Rivera-Hernández<sup>3</sup>, N. Stein<sup>4</sup>, J.K. Van Beek<sup>5</sup>.  
6 <sup>1</sup> Texas A&M University, Department of Geology and Geophysics, 3115 TAMU, College Station,  
7 TX, 77843, USA. <sup>2</sup> Department of Astronomy and Planetary Sciences - College of Engineering,  
8 Forestry, & Natural Sciences Northern Arizona University - Flagstaff, AZ 86011-6010, USA. <sup>3</sup>  
9 Department of Earth Sciences, Dartmouth College, 6105 Fairchild Hall, Hanover, NH 03755,  
10 USA. <sup>4</sup> California Institute of Technology, Division of Geological and Planetary Sciences, CA,  
11 USA. <sup>5</sup> Malin Space Science Systems, San Diego, California, USA. Corresponding author:  
12 mnachon@tamu.edu.  
13

14 This paper is a non-peer reviewed preprint submitted to EarthArXiv.  
15 A version of this paper has been submitted to the journal Earth and Space Science.  
16  
17  
18

19 **Key Points**

- 20       • Mastcam images from the Curiosity rover are available online but lacked a public method  
21       to be placed back in the Mars orbital context.
- 22       • This procedure permits to generate Mastcam image viewsheds: it identifies on Mars  
23       orbital view the terrains visible in a given Mastcam image.
- 24       • This procedure uses ArcGIS® and publicly available Mars datasets.  
25

26  
27 **Abstract**

28 The Mastcam (Mast Camera) instrument onboard the NASA Curiosity rover provides an exclusive  
29 view of Mars: the color high-resolution Mastcam images allow users to study Gale crater's  
30 geological terrains and landscapes along the rover path. This view from the ground complements  
31 the spatially broader view provided by spacecrafts from orbit. However, for a given Mastcam  
32 image, it can be challenging to locate on the orbital view the corresponding terrains. No method  
33 for collocating Mastcam onto orbital images had been made publicly available. The procedure  
34 presented here allows users to generate Mastcam viewsheds, using the ArcGIS® software and its  
35 built-in Viewshed tool as wells as Mars datasets exclusively public. This procedure locates onto  
36 Mars orbital view the terrains that are observed in a given Mastcam image. Because this procedure  
37 uses public datasets, it is applicable to the Mastcam images already available online and to the  
38 upcoming ones, as collected along Curiosity rover's path. In addition, this procedure constitutes  
39 material for a pedagogic GIS project in Geosciences or Planetary Sciences, to handle Mars datasets  
40 both orbital and from the Curiosity rover.

41	<b>Table of contents</b>	
42	1. Introduction .....	3
43	1.1. Complementarity of ground and orbital views of Mars for geological studies .....	3
44	1.2. Placing Mastcam images from the Curiosity rover into the Mars orbital context.....	3
45	2. Datasets and software .....	5
46	2.1. Mastcam datasets .....	5
47	2.2. Orbital datasets and Curiosity rover’s path at Gale crater .....	6
48	2.3. ArcGIS®: GIS project and use of the Viewshed tool .....	6
49	3. Mastcam image viewshed procedure: overview and illustrative example .....	7
50	Step 1: Gather and organize Mars public datasets .....	7
51	Step 2: Extract and calculate Mastcam image properties.....	8
52	Step 3: Generate the Mastcam image viewshed with the ArcGIS® Viewshed tool .....	12
53	4. Conclusions and perspectives .....	15
54		
55		

## 56 1. Introduction

### 57 1.1. Complementarity of ground and orbital views of Mars for geological 58 studies

59 Images of Mars's terrains and landscapes collected via the successive space missions keep refining  
60 our view and understanding of the red planet. Historically, the images collected with spacecrafts  
61 (e.g. Mariner 4 flyby in 1965) have offered a spatially-wide view of Mars that later got  
62 complemented by higher-resolution images collected from the ground with landers (e.g. Viking 1  
63 landed in 1976 and InSight in 2018) and then rovers (Pathfinder landed in 1997, Spirit and  
64 Opportunity in 2004 and Curiosity in 2012). Orbital images have also been used for landing site  
65 selection of ground missions, and also to guide the path and the daily operations of rovers once  
66 landed, e.g. the Curiosity rover [Stack et al., 2016]. Because both orbital and ground views offer  
67 complementary information, their coupling is key for optimizing the study and interpretation of  
68 geological terrains and landscapes.

69 Orbital images, on one hand, are particularly useful for capturing a global or regional to local  
70 context, down to the meter scale, that cannot be provided by a typical rover visual range [Stack et  
71 al., 2016]. In particular, detailed orbital mapping based on high-resolution image datasets provides  
72 critical context for the more detailed rover measurements. However, the coverage of the surface  
73 of Mars by the most recent orbital imagers does not yet encompass the entire planet: the High  
74 Resolution Imaging Science Experiment (HiRISE) onboard the spacecraft Mars Reconnaissance  
75 Orbiter mapped ~0.55% of the surface at a scale from 25 to 60 cm/pixel, between October 2006  
76 and December 2008 [McEwen et al., 2010]. Moreover, despite the increased sophistication of  
77 recent orbiter image-based geologic mapping efforts, the interpretation of Mars's geology based  
78 exclusively on orbital image datasets still carries considerable uncertainties [Stack et al., 2016]:  
79 three-dimensional outcrop exposures are difficult to observe in orbital data, thus limiting the  
80 geological interpretation of outcrop exposed as observed in orbital data. Also, even 25 cm/pixel  
81 HiRISE images provide limited to no information about the small-scale textural characteristics of  
82 geological material, which are critical for making depositional interpretations.

83 Ground images, on the other hand, offer a higher-resolution view of Martian terrains and provide  
84 "ground-truth" observations for orbital images. Ground-based images are needed to investigate the  
85 small-scale textural characteristics of outcrops, such as grain-size, lithology, internal sedimentary  
86 structures, or bedding styles, which are key for making depositional interpretations and  
87 paleoenvironmental reconstruction [e.g. Stack et al., 2016; Banham et al., 2018; Lewis and Turner,  
88 2019; Stein et al., 2020]. However, *in-situ* observations of the Martian surface are limited to the  
89 locations visited by ground missions (8 landers and rovers, as of 2020).

90 In conjunction with each other, orbital and *in situ* observations provide an ideal, complementary  
91 approach to investigate a planetary surface. Because they offer complementary information, their  
92 coupling is key for optimizing the study and interpretation of geologic terrains and landscapes.  
93 Such complementary of datasets is also used for rover navigation, in particular to obtain precise  
94 rover localization [e.g. Parker et al., 2013; Weishu Gong, 2015] and to assist selection of rovers'  
95 routes (e.g. minimizing traverses across wheel-damaging terrains [Arvidson et al., 2017]).

## 1.2. Placing Mastcam images from the Curiosity rover into the Mars orbital context

Among the cameras present onboard the Curiosity rover from the NASA Mars Science Laboratory (MSL) mission, the Mastcam imagers provide an exclusive high-resolution color view of Mars (Fig. 1A). Mastcam (Mast Cameras) consists of a pair of color CCD imagers (Mastcam Left and Mastcam Right) mounted on the rover's mast at a height of 1.97 meters [Bell et al., 2017; Malin et al., 2017] (Fig. 1C). Mastcam Right (MR) has a 100-mm focal length and a field of view of  $6.8^{\circ} \times 5.1^{\circ}$  and Mastcam Left (ML) has a 34-mm focal length and a field of view of  $20^{\circ} \times 15^{\circ}$  [Bell et al., 2017; Malin et al., 2017]. MR and ML can respectively achieve pixel scales of  $\sim 150 \mu\text{m}$  and  $\sim 450 \mu\text{m}$  from 2 meters [Malin et al., 2017]. The Mastcam images allow for fine-scale study of the properties of outcrops and rocks [e.g. Le Deit et al., 2016; Stein et al., 2018], landscape physiography [e.g. Grotzinger et al., 2015], and properties sand [e.g. Bridges et al., 2017; Ewing et al., 2017]. They also provide visual context for the compositional analyses from Curiosity's instruments such as ChemCam (Chemistry and Camera) and APXS (Alpha Particle X-Ray Spectrometer) [e.g. Wiens et al., 2017; Nachon et al., 2017; Thompson et al., 2016].

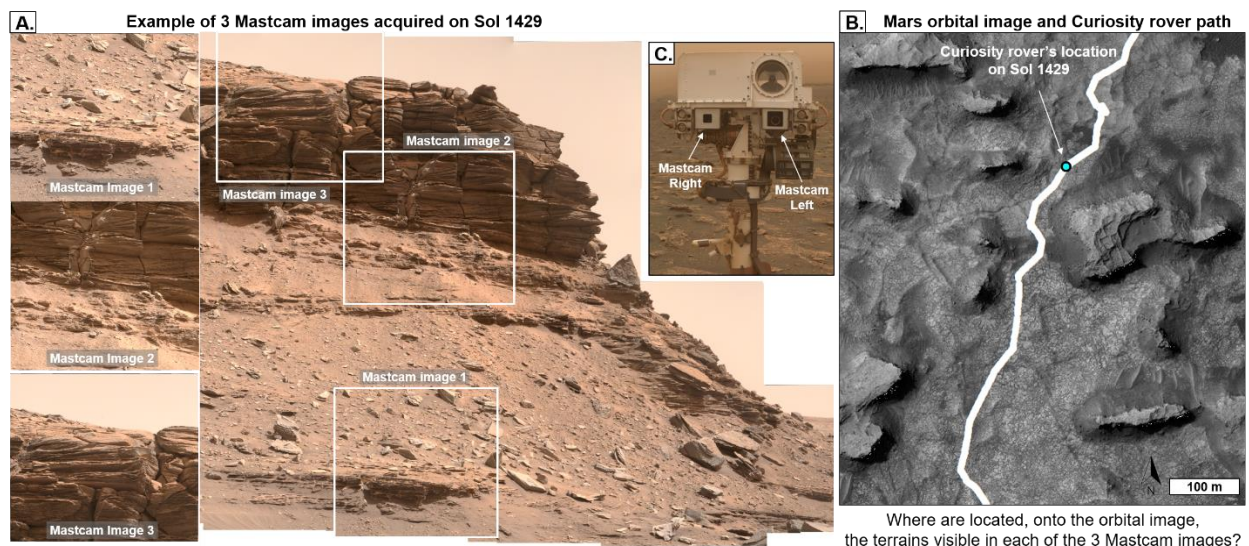


Figure 1: Illustration of the challenge of collocating Mastcam and orbital images, based on public datasets. **A.** Example of 3 individual Mastcam images. Combined with other Mastcam images acquired on that Sol to generate a mosaic. **B.** Mars orbital view of Curiosity rover's location on Sol 1429. **C.** Mastcam imagers on Curiosity's mast.

Mastcam images have been used alongside orbital images in several geologic studies of Gale crater's terrains, such as: (1) locating and mapping contacts between geologic units or members to establish the stratigraphy of the terrains (e.g. Sheepbed mudstone and overlying Gillespie Lake sandstone in the Yellowknife Bay formation [McLennan et al., 2014]); (2) interpreting the geologic origin of outcrops (e.g. aeolian Stimson formation [Banham et al., 2018]); (3) mapping geologic features too small to be observed from orbit, to determine their spatial and stratigraphic distribution in the different geologic units (e.g. light-toned veins [Nachon et al., 2017] and concretions [Sun et al., 2019]). As of January 2020, over 130,000 raw Mastcam images have been acquired (along the 20 km long path of the Curiosity rover) and have been publicly released (Table 1).

126

127 Despite the mentioned studies, no method for collocating Mastcam and orbital images has been  
128 made publicly available, presenting a roadblock to synchronous use of these datasets. As a result,  
129 geologic features present within Mastcam images can be challenging to identify within an orbital  
130 image of Gale crater, when using only public data. Most of Mastcam images contain geologic  
131 features tens to hundreds of meters away from the rover’s traverse. It is difficult to deduce the  
132 spatial scale and location of features in these Mastcam images due to the combination of  
133 foreshortening and the lack of reference features. For example, the terrain imaged on Mastcam  
134 image 3 (Fig. 1A) acquired on Sol (Martian day) 1429 appears to depict the top of a butte; yet, on  
135 the orbital image of the rover on that Sol (Fig 1B), the location (how far from the rover, and in  
136 which direction) and the spatial extend of this terrain is not straightforward to identify..

137

138 Herein we describe a procedure that uses ArcGIS® and public Mars datasets to locate, onto Gale  
139 crater orbital view, the terrains that are visible in a given Mastcam image. By successfully  
140 correlating *in situ* and remote observations of Gale crater, Mars, we provide the Geoscience and  
141 Planetary Science communities access to tools for investigating Martian surface processes and  
142 geologic history.

## 143 **2. Datasets and software**

144 The datasets used are publicly available online (Table 1).

Dataset	File name	Source link
Mastcam images and associated labels. <i>See section 2.1</i>	Images are in .IMG format. Labels are in .LBL format.	<a href="https://pds-imaging.jpl.nasa.gov/volumes/msl.html">https://pds-imaging.jpl.nasa.gov/volumes/msl.html</a>  Under successive volumes (MSLMST_00NN, where NN currently goes from 01 to 19), and in the “DATA” folders.
Gale crater orbital orthophoto mosaic. (“Gale crater mosaic”) <i>See section 2.2</i>	MSL_Gale_Orthophoto_Mosaic_25cm_v3 <a href="#">Original</a> 23 GB. File is in .tif format.	<a href="http://astrogeology.usgs.gov/search/map/Mars/MarsScienceLaboratory/Mosaics/MSL_Gale_Orthophoto_Mosaic_10m_v3">http://astrogeology.usgs.gov/search/map/Mars/MarsScienceLaboratory/Mosaics/MSL_Gale_Orthophoto_Mosaic_10m_v3</a>
Gale crater DEM (Digital Elevation Model). <i>See section 2.2</i>	MSL_Gale_DEM_Mosaic_1m_v3 <a href="#">Original</a> 3.6 GB. File is in .tif format.	<a href="http://astrogeology.usgs.gov/search/map/Mars/MarsScienceLaboratory/Mosaics/MSL_Gale_DEM_Mosaic_10m">http://astrogeology.usgs.gov/search/map/Mars/MarsScienceLaboratory/Mosaics/MSL_Gale_DEM_Mosaic_10m</a> .
Rover path localization table. <i>See section 2.2</i>	Table “ <i>localized_interp.csv</i> ”.	<a href="https://pds-imaging.jpl.nasa.gov/data/msl/MSLPLC_1XXX/DATA/LOCALIZATIONS/">https://pds-imaging.jpl.nasa.gov/data/msl/MSLPLC_1XXX/DATA/LOCALIZATIONS/</a>

145 *Table 1: Mars datasets used and their respective public sources.*

146

### 147 **2.1. Mastcam datasets**

148 Mastcam images and metadata are posted on the NASA PDS (Planetary Data System),  
149 Cartography and Imaging Sciences Node (Table 1) under successive volumes of conventional  
150 name “MSLMST\_00NN” (where NN currently goes from 01 to 22), and in the “DATA” folders.



151 Mastcam data is released on a regular schedule (every 4 to 6 months, see <http://pds-geosciences.wustl.edu/missions/msl/>). It is also available via the MSL Analyst's Notebook (<https://an.rsl.wustl.edu/msl/>) that provides an interactive way of visualizing Curiosity's successive locations and of accessing the data collected by the rover on each Sol.

155

156 Mastcam data naming convention uniquely identifies an image or metadata product: in particular, the first 4 digits correspond to the Sol during which the image was acquired, and the letters in position 5 and 6 correspond to the camera name: "MR" for Mastcam Right or "ML" for Mastcam Left [MMM DPSIS 2013, Table 3.4-1, Section 3.4].

160

### 161 ***Mastcam images***

162 The Mastcam images on the PDS are in ".IMG" format (binary image data) [MMM DPSIS 2013]. Here we work with Mastcam RDR (Reduced Data Record) images: they have been decompressed, radiometrically calibrated, color corrected or contrast stretched, and linearized: this is reflected on their naming convention, where the digits in position 27 to 30 state "DRCL" [MMM DPSIS 2013]. For example, image [1429MR0070680050702586E01\\_DRCL.IMG](https://pds-imaging.jpl.nasa.gov/data/msl/MSLMST_0014/DATA/RDR/SURFACE/1429/) posted on [https://pds-imaging.jpl.nasa.gov/data/msl/MSLMST\\_0014/DATA/RDR/SURFACE/1429/](https://pds-imaging.jpl.nasa.gov/data/msl/MSLMST_0014/DATA/RDR/SURFACE/1429/).

168

### 169 **Mastcam labels: images metadata**

170 For each Mastcam image, its corresponding metadata is in an associated label (a text file in ".LBL" format) [MMM DPSIS 2013, Appendix A]. In particular, labels include information about images properties, and about the location of the rover when the image was acquired.

173

## 174 **2.2. Orbital datasets and Curiosity rover's path at Gale crater**

175 The mosaic covering the Curiosity rover's path area within Gale Crater is available on the USGS website (Table 1). It was assembled from High Resolution Imaging Science Experiment (HiRISE) images from Mars Reconnaissance Orbiter (MRO) [Calef and Parker, 2016]. The associated DEM (Digital Elevation Model) provides the topography of the terrains, at 1m/pixel resolution [Calef and Parker, 2016]. It was built from HRSC (High Resolution Stereo Camera) data from the ESA Mars Express spacecraft, CTX (Context Camera) and HiRISE data from MRO spacecraft, and MOLA (Mars Orbiter Laser Altimeter) data from MGS (Mars Global Surveyor) spacecraft [Calef and Parker, 2016]. Both the mosaic and the DEM are raster graphics images, in .TIF format.

183 Curiosity rover's successive locations on each Sol are publicly available as a plain text table (in .CSV format) on the PDS (Table 1), where they are expressed both in rover coordinate frame ("Site" and "Drive", defined as successive position of the rover [MSL Coordinate Systems, 2013]) and in the corresponding latitude and longitude values.

187

## 188 **2.3. ArcGIS®: GIS project and use of the Viewshed tool**

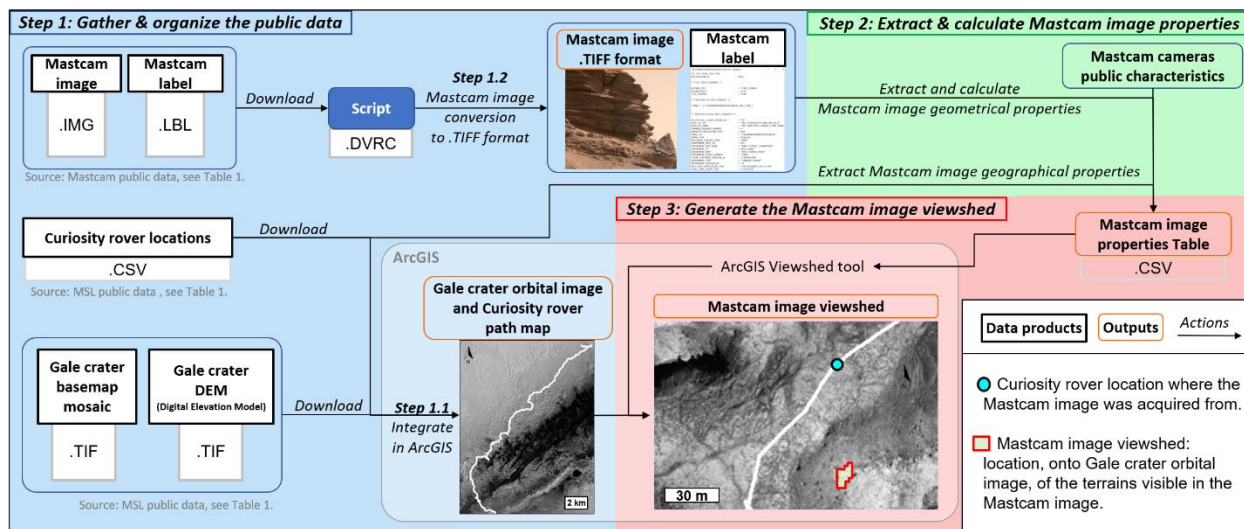
189 The software ArcGIS® (version 10.5) is here used to build an interactive GIS (geographic information system) project that displays the rover path onto the Gale crater orbital mosaic and DEM.

192

213 The built-in ArcGIS® Viewshed tool uses the location of an observer on a DEM to identify raster  
 214 cells that lie within and outside of the field of view of the observer at their precise location..  
 215 Because this tool allows to limit the region of the raster inspected, we use it to identify on the Mars  
 216 orbital data the terrains that are visible (1) from the position of the rover onto the Gale crater DEM  
 217 at the time a given Mastcam image was acquired and (2) from the Mastcam imager point of view  
 218 at that given time (Section 3, Step 3). This process highlights on orbital view the area(s) that  
 219 correspond to what is observed in the Mastcam image. We term these highlighted regions  
 220 “Mastcam image viewsheds”.

### 221 3. Mastcam image viewshed procedure: overview and illustrative 222 example

223 This section presents our procedure for generating a Mastcam image viewshed in ArcGIS®, using  
 224 data exclusively public. This allows to locate onto the Gale crater orbital view the terrains visible  
 225 in a given Mastcam image (Fig. 2). The main steps of the procedure are: (1) gather the Mars public  
 226 datasets and organize a GIS project to create a map of the Curiosity rover path as seen from orbit;  
 227 (2) extract and calculate Mastcam image characteristics; (3) feed these characteristics into the GIS  
 228 project and the ArcGIS® Viewshed tool. [This procedure overview is furthermore illustrated by an](#)  
 229 [example application \(text in blue\) based on Mastcam image](#)  
 230 [1429MR0070680170702598E01\\_DRCL](#). Extended descriptions of the procedure steps are  
 231 provided in the supporting information and referenced along the manuscript.



214  
 215 *Figure 2: Flowchart of the procedure to generate a Mastcam image viewshed in ArcGIS® using*  
 216 *data exclusively public. This allows to locate on Mars orbital view the terrains that are visible in*  
 217 *a given Mastcam image.*

#### 219 Step 1: Gather and organize Mars public datasets

220 Step 1 first consists in downloading the Mars orbital and Mastcam datasets (Step 1.1). We also  
 221 include an automated method for converting Mastcam images from .IMG into .TIFF format (Step  
 222 1.2). Step 1.3 is to integrate the Curiosity rover traverse map in ArcGIS®.

223

224 **Step 1.1: Download datasets**

225 All datasets use here are publicly available for download and include the Mastcam data (images  
226 and associated labels), Gale crater orthophoto mosaic, Gale crater DEM, and the Curiosity rover  
227 path localization table (Section 2 and Table 1).

228 **Step 1.2 (Optional): Mastcam images conversion to .TIFF format**

229 To convert the Mastcam images available online on the PDS (Table 1) from the binary format  
230 “.IMG” into “.TIFF” format, and automate this process to various Mastcam images, we provide a  
231 script (in DaVinci language) in the supplementary material. This format conversion allows the  
232 images to be visualized via more basic computer programs.

233

234 **Step 1.3: Build the Curiosity rover traverse map in ArcGIS®**

235 In ArcMap, import the Gale crater mosaic as well as the DEM covering the Curiosity rover’s path  
236 area within Gale Crater, and the table of successive locations of Curiosity.

1.3.1 Launch ArcMap, select a new document, and save it.

1.3.2 To display the Gale crater imagery mosaic and the DEM:

- Download the Gale crater mosaic and the Gale DEM (see Table 1).
- In the ArcMap project, click *File/Add data/ Add data*. Select the Gale crater mosaic. Then do the same for adding the DEM.

1.3.3 To display the rover path in the ArcMap project:

- Download the rover path localization table (“localized\_interp.csv”) (see Table 1). The columns that contain information directly relevant for this ArcGIS® project are: (1) the rover coordinates columns (“planetocentric\_latitude” and “longitude”, as well as “site” and “drive”); (2) the elevation of the rover at a given location (“elevation”); (3) the corresponding martian days (“Sols”) for each of the rover localizations.
  - In the ArcMap project, click *File/Add data/Add XY Data*. In the window that appears, choose the “rover\_path” table, and specify the fields for the X,Y and Z coordinates as follow: for X field select “longitude”; for Y field select “planetocentric\_latitude”; for Z field select “sol”.
  - In the “Coordinate System and Input Coordinates”, click on “Edit”. Under the “Geographic Coordinate Systems/Solar System/Mars” folders, select “Mars 2000”.

237

238

239 **Step 2: Extract and calculate Mastcam image properties**

240 For a given Mastcam image, Step 2 consists in extracting and calculating its geometrical and  
241 geographical properties that will be used (in Step 3) to ingest into the ArcGIS® Viewshed tool.

242

243 **Step 2.1: Extract Mastcam image geographical properties**

244 The geographical properties needed correspond to the location of the rover at the time the Mastcam  
245 image was acquired. A first order information about this location is provided by the Sol number,  
246 which is indicated by the first 4 digits of the image ID (section 2.1). Further information about this  
247 location is included in the Mastcam image label file (under the subsection “/\* Identification Data  
248 Elements \*/”), as expressed in the rover coordinate frame: the “*SITE*” and “*DRIVE*” values  
249 (Section 2.2.). To obtain the actual coordinates corresponding to this location, we use the “Rover



250 path localization table” (Table 1) that for each combination of “Site” and “Drive” values, provides  
 251 the corresponding Mars coordinates (latitude and longitude).  
 252 For example, the label file of Mastcam image 1429MR0070680170702598E01\_DRCL indicates  
 253 that “SITE” value is 56 and “DRIVE” value is 1632. In the “Rover path localization table”, for  
 254 these values, the planetocentric latitude and the longitude are respectively  $-4.687932383^\circ$  and  
 255  $137.35402705^\circ$ .

	A	B	C	D	E	F	G	H	I	J	K	L
1	frame	site	drive	pose	landing_x	landing_y	landing_z	northing	easting	planetoc	planetode	longitude
16428	ROVER	56	1608	-1	-5834.58	-5190.34	-93.087	-277874	8141621	-4.6879	-4.74332	137.354
16429	ROVER	56	1614	-1	-5834.67	-5190.46	-93.101	-277874	8141621	-4.6879	-4.74333	137.354
16430	ROVER	56	1620	-1	-5835.44	-5191.45	-93.211	-277875	8141620	-4.68791	-4.74334	137.354
16431	ROVER	56	1626	-1	-5836.16	-5192.37	-93.299	-277875	8141619	-4.68793	-4.74335	137.354
16432	ROVER	56	1632	-1	-5836.51	-5192.82	-93.34	-277876	8141618	-4.68793	-4.74336	137.354
16433	ROVER	56	1638	-1	-5836.8	-5193.15	-93.366	-277876	8141618	-4.68794	-4.74336	137.354
16434	ROVER	56	1644	-1	-5837.1	-5193.37	-93.408	-277876	8141618	-4.68794	-4.74337	137.354
16435	ROVER	56	1650	-1	-5837.91	-5193.91	-93.457	-277877	8141617	-4.68796	-4.74338	137.354
16436	ROVER	56	1656	-1	-5838.73	-5194.45	-93.486	-277878	8141617	-4.68797	-4.7434	137.354
16437	ROVER	56	1662	-1	-5839.55	-5195.01	-93.505	-277879	8141616	-4.68798	-4.74341	137.354
16438	ROVER	56	1668	-1	-5840.35	-5195.55	-93.528	-277880	8141616	-4.688	-4.74342	137.354
16439	ROVER	56	1674	-1	-5841.16	-5196.1	-93.56	-277880	8141615	-4.68801	-4.74344	137.354
16440	ROVER	56	1680	-1	-5841.98	-5196.66	-93.585	-277881	8141615	-4.68802	-4.74345	137.354
16441	ROVER	56	1686	-1	-5842.59	-5197.06	-93.609	-277882	8141614	-4.68804	-4.74346	137.354
16442	ROVER	56	1692	-1	-5843.42	-5197.55	-93.638	-277883	8141614	-4.68805	-4.74348	137.354
16443	ROVER	56	1698	-1	-5844.24	-5198.03	-93.677	-277884	8141613	-4.68806	-4.74349	137.354
16444	ROVER	56	1704	-1	-5845.05	-5198.52	-93.722	-277884	8141613	-4.68808	-4.7435	137.354
16445	ROVER	56	1710	-1	-5845.87	-5199	-93.782	-277885	8141612	-4.68809	-4.74352	137.354
16446	ROVER	56	1716	-1	-5846.46	-5199.41	-93.83	-277886	8141612	-4.68811	-4.74353	137.354
16447	ROVER	56	1722	-1	-5847.25	-5199.93	-93.879	-277887	8141611	-4.68811	-4.74354	137.354
16448	ROVER	56	1728	-1	-5847.86	-5200.33	-93.895	-277887	8141611	-4.68812	-4.74355	137.354
16449	ROVER	56	1734	-1	-5848.65	-5200.84	-93.914	-277888	8141610	-4.68814	-4.74356	137.354

256  
 257  
 258  
 259  
 260  
 261  
 262  
 263  
 264  
 265  
 266  
 267  
 268  
 269  
 270  
 271  
 272  
 273  
 274  
 275  
 276

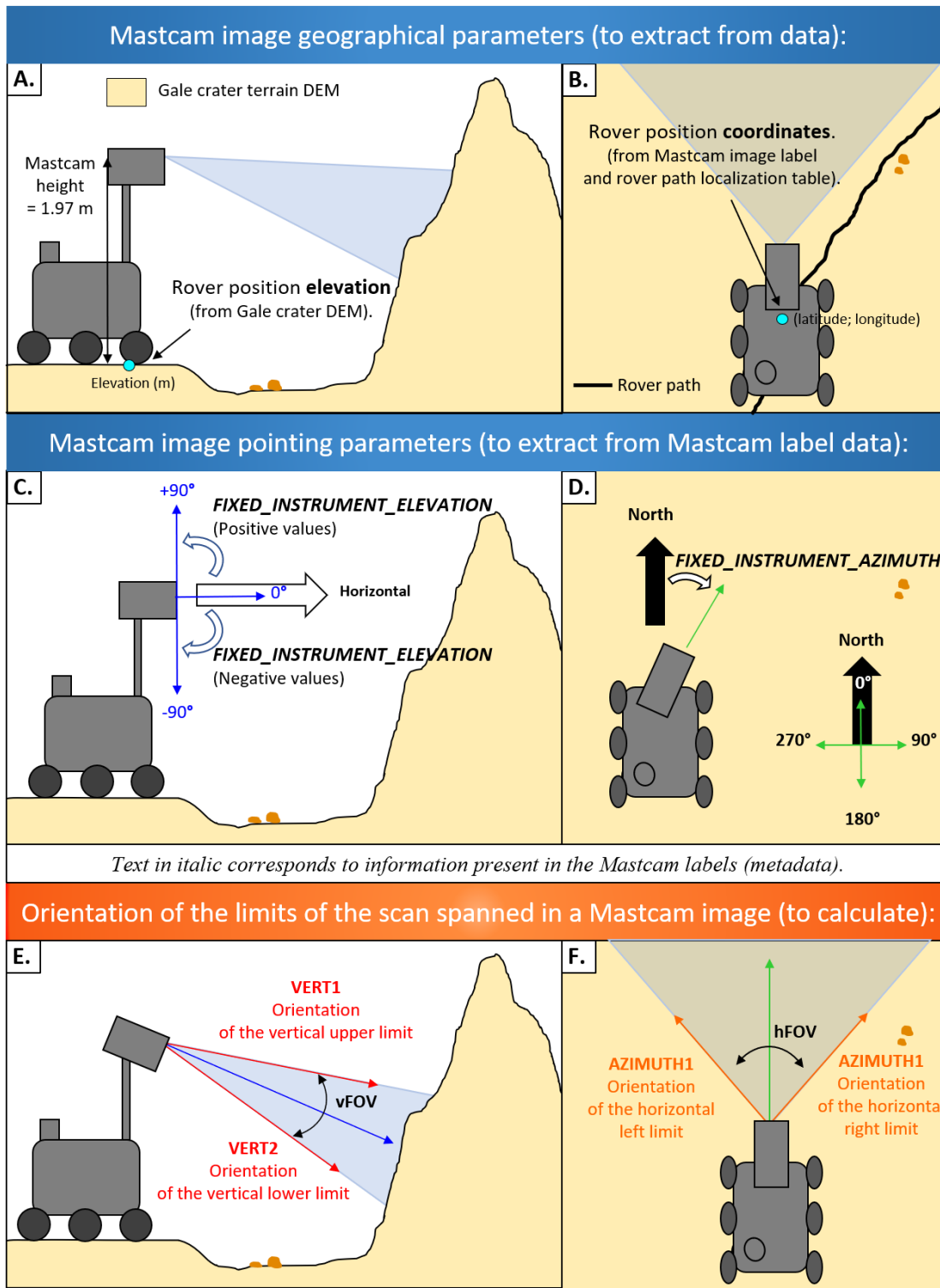
## Step 2.2: Calculate Mastcam image geometrical properties

The geometrical properties correspond to the vertical and horizontal limits of the scan spanned in a given Mastcam image, from the rover location. To calculate them, 2 categories of information are used: (1) the fixed field of view of the Mastcam camera (Right of Left) used to collect the image; (2) the orientation of the Mastcam instrument (the vertical and horizontal angles it was pointing at) when the image was acquired.

First, the Mastcam Right and Left span a fixed FOV of respectively  $6.8^\circ \times 5.1^\circ$  and  $20^\circ \times 15^\circ$  [Bell et al., 2017; Malin et al., 2017]. The vertical and horizontal fields of view (vFOV and hFOV) correspond respectively to the angle of the view up-to-down, and of the view side-to-side. For a given Mastcam image, which of the Mastcam cameras (Right or Left) was used to collect the image is indicated in the Mastcam data ID (section 2.1). Mastcam image with ID “1429MR0070680050702586E01\_DRCL” corresponds to a Mastcam Right image. Thus, its horizontal field of view (hFOV) is  $6.8^\circ$ , and vertical field of view (vFOV) is  $5.1^\circ$ .

Second, the Mastcam instrument can be pointed vertically and horizontally at variable degrees, depending on the analyses wanted by the MSL Team along the Curiosity rover traverse. The pointing parameters under which a given Mastcam image was acquired are indicated in the

277 Mastcam label file (under the subsection “/\* Derived Data Elements \*/”) by the following 2  
278 parameters:  
279 - The “*FIXED\_INSTRUMENT\_AZIMUTH*” (Fig. 3D) is the angle of the pointing direction of  
280 the Mastcam instrument with respect to the North. It is measured positively in the clockwise  
281 direction [MMM DPSIS 2013]. An angle of 90° corresponds to a pointing of the camera towards  
282 the East.  
283 - The “*FIXED\_INSTRUMENT\_ELEVATION*” (Fig. 3C) is the vertical angle of the pointing  
284 direction of the Mastcam instrument. It is measured from the plane which is perpendicular to the  
285 local gravity vector and which intersects the elevation axis around which the instrument rotates  
286 [MMM DPSIS 2013]. An angle of 0° corresponds to an horizontal pointing of the camera.  
287 For image 1429MR0070680050702586E01\_DRCL, the *FIXED\_INSTRUMENT\_AZIMUTH*  
288 value indicated in the label is 174.6128, and the *FIXED\_INSTRUMENT\_ELEVATION* is  
289 11.4751. This indicates that the Mastcam instrument was pointed at 8.345 ° above the horizontal  
290 plane, and in a direction East/South-East, when the image was acquired.  
291



292  
293  
294  
295  
296  
297  
298  
299  
300

Figure 3: Schematic of the geometrical and geographical properties of a Mastcam image, used to create a corresponding viewshed. Geographical properties include the rover location's elevation (A.) and coordinates at the time the Mastcam image was acquired (B.). The fixed instrument elevation (blue arrow) is the vertical angle of the pointing direction of the Mastcam camera (C.) The fixed instrument azimuth (green arrow) is the angle of the pointing direction of the Mastcam instrument with respect to the North (C.). Mastcam image vertical limits (red arrows) are the angles of the view limits up-to-down (E.), and the horizontal limits (orange arrows) is the orientation of the view limits side-to-side (F.).

301  
302 To calculate the orientation of the limits of the scan spanned in a given Mastcam image, we first  
303 address the vertical (upper and down) limits, and second the horizontal (left and right) limits.

304  
305 First, the vertical orientation limits of the Mastcam image scan are defined with respect to the  
306 horizontal plane and are here called VERT1 and VERT2 (Fig. 3E). They are expressed in degrees  
307 between 90 and -90°, with positive values representing angles above the horizontal plane.

308 Vertical upper limit:  $VERT1 = Fixed\_instrument\_elevation + \left(\frac{vFOV}{2}\right)$

309 and

310 Vertical lower limit:  $VERT2 = Fixed\_instrument\_elevation - \left(\frac{vFOV}{2}\right)$

311  
312 For image 1429MR0070680050702586E01\_DRCL:

313  $VERT1 = Fixed\_instrument\_elevation + \left(\frac{vFOV}{2}\right) = 11.4751 + \left(\frac{5.1}{2}\right) = 14.0251$

314 and

315  $VERT2 = Fixed\_instrument\_elevation - \left(\frac{vFOV}{2}\right) = 11.4751 - \left(\frac{5.1}{2}\right) = 8.9251$

316 The vertical scan limits spanned in this image range from 8.9251° to 14.0251° above the  
317 horizontal plane.

318  
319 Second, the horizontal angle limits are defined with respect to the North and are here called  
320 AZIMUTH1 and AZIMUTH2 (Fig. 3F). The sweep proceeds in a clockwise direction from the  
321 first azimuth to the second. The values for the angle are given in degrees from 0 to 360°, with 0°  
322 oriented to North.

323 Horizontal left limit:  $AZIMUTH1 = Fixed\_instrument\_azimuth - \left(\frac{hFOV}{2}\right)$

324 and

325 Horizontal right limit:  $AZIMUTH2 = Fixed\_instrument\_azimuth + \left(\frac{hFOV}{2}\right)$

326  
327 For image 1429MR0070680050702586E01\_DRCL:

328  $AZIMUTH1 = Fixed\ instrument\ azimuth - \left(\frac{hFOV}{2}\right) = 174.6128 - \left(\frac{6.8}{2}\right) = 171.2128$

329 and

330  $AZIMUTH2 = Fixed\ instrument\ azimuth + \left(\frac{hFOV}{2}\right) = 174.6128 + \left(\frac{6.8}{2}\right) = 178.0128$

331 The horizontal scan limits spanned in this image range from 171.2128° to 178.0128° with respect  
332 to North, which corresponds to a South/South-East direction.

333

334

335 **Step 3: Generate the Mastcam image viewshed with the ArcGIS® Viewshed**  
336 **tool**

337 We use the fact that in ArcGIS® the built-in Viewshed tool allows to identify the cells of a raster  
338 that can be seen from a given observation location (Section 2.2). For generating a Mastcam image  
339 viewshed, the information to ingest into the ArcGIS® Viewshed tool is:

- 340 - The input raster, that corresponds to the Gale crater DEM (Section 2.2), to provide both the  
 341 elevation of rover location from where a given Mastcam image was taken, and the  
 342 topography of the surrounding terrains.
- 343 - The point observer feature, that here corresponds to a shapefile comprising the Mastcam  
 344 image properties extracted and calculated in step 2.2.: the rover coordinates from where  
 345 the Mastcam image was collected as well as the values for the following Viewshed tool build-in  
 346 items [ArcGIS® “Using Viewshed and Observer Points for visibility analysis”]:
- 347 • OFFSETA: indicates the “vertical distance in surface units to be added to the z-value  
 348 of the observation point”. Here it corresponds to the height of the Mastcam instrument  
 349 with respect to the Mars ground, i.e. 1.97 meters [Bell et al., 2017].
  - 350 • VERT1 and VERT2 that define the vertical angle limits to the scan.
  - 351 • AZIMUTH1 and AZIMUTH2 that define the horizontal angle limits to the scan.
- 352

**3.1** Create an excel table with the viewshed items corresponding to the Mastcam image:  
 The table should include 7 columns (latitude, longitude, OFFSETA, AZIMUTH1, AZIMUTH2, VERT1 and VERT2) and 2 rows (the first one with the names of the items, the second with the corresponding values of these items). The names of the items should be kept as is: they are parameters used by the tool. Save the table in format .xls Excel2003.

**3.2** Load the excel table into ArcGIS® and convert into shapefile  
 Go to: **File/Add Data/Add XY Data** and select the table. Once it is loaded, in the Table of Contents window right click on it. Click **Data/Export Data**. In the Export Data window that appears, under “Output feature class” select “Save as type” as “Shapefile”. Click ok.

**3.3** Apply the ArcGIS® viewshed tool:

- In the Menu Customize/Toolbars, verify that the Spatial Analyst is checked.
- Go to the menu Geoprocessing, click on ArcToolbox. Find the “Viewshed” tool, under Visibility. Or in the Search For Tools window, search for viewshed.
- Launch the Viewshed tool window:

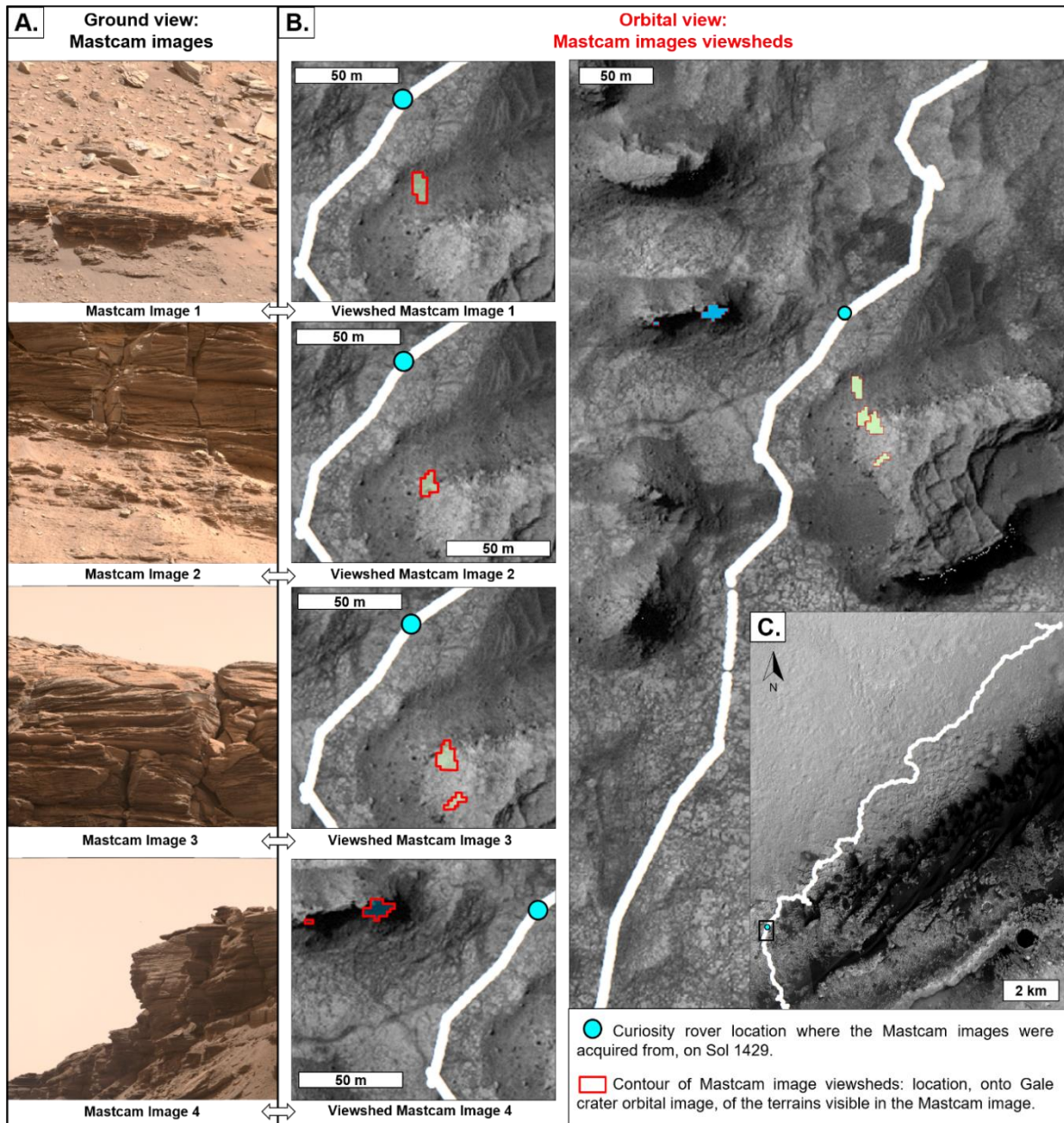
As Input raster: select the Gale crater DEM (MSL\_Gale\_DEM\_Mosaic\_1m, ref). As Input point: select the shapefile created above. As Output raster: select a path where to store the viewshed, and name it. Click on *Environments*. Under the Workspace menu, specify the folder where data is. Under the Processing Extent extend menu, you can select “Same as display”, in order to make the Viewshed tool run for the current view displayed in your ArcMap project. This is a way to accelerate the calculations.

**3.4** The output will typically display the terrains “Visible” (the viewshed) in green, and in pink the terrains that are “not visible” (that are not the viewshed). The pink color can be set to “No color” in order to only left highlighted the terrains that correspond to the viewshed, while still being able to visualize the terrains surrounding: right click on the “No Visible” symbol, select “No color”. Also, the transparency of the viewshed can be tuned (ArcGIS® source: <https://desktop.ArcGIS.com/en/arcmap/10.3/map/working-with-layers/how-to-set-layer-transparency.htm>): right click on the “Visible” layers, go to *Layer Properties* and *Set transparency*.

353  
 354



355 Examples of 4 Mastcam image viewsheds (Fig. 4B) generated for 4 Mastcam images acquired on  
 356 Sol 1429 (Fig. 4A) are presented. Mastcam images 3 and 4 display terrains corresponding to  
 357 outcrops tops. Their respective viewsheds show they correspond to 2 distinct buttes. Mastcam  
 358 image 1 corresponds to a lower part of the butte slope, compared to the other 3 images. It  
 359 corresponding viewshed indeed appears closer to the rover location at the moment the Mastcam  
 360 image was acquired (blue dot). Finally, Mastcam images 2 and 3 slightly overlap (as visible in the  
 361 Mastcam mosaic on Fig 1A), and this configuration is captured in the viewsheds.  
 362



363  
 364 *Figure 4: Illustration of our procedure for generating Mastcam image viewsheds. A. Four*  
 365 *Mastcam images, acquired on Sol 1429. B. Their respective viewsheds. Viewsheds 3 and 4 both*  
 366 *correspond to two areas, because their corresponding Mastcam images 3 and 4 both display*

367       terrains with “false horizons”: a part of the butte, distinct than the one in the foreground, is  
368               present in the images background. C. Orbital view of the Curiosity rover’s path.

#### 369 **4. Conclusions and perspectives**

370 Here is provided a procedure that for a given Mastcam image acquired with the Curiosity rover,  
371 locates on Mars orbital view the terrains that are visible in this Mastcam image. Using the  
372 ArcGIS® software (to build a GIS project and to use the build-in ArcGIS® Viewshed tool) and  
373 Mars datasets exclusively public, the procedure allows users to place the color higher-resolution  
374 Mastcam image into the spatially-broader orbital context, and thus allow coupling both the ground  
375 and orbital view of given terrains in Gale crater. This is particularly relevant for analyzing and  
376 interpreting the geological terrains along the rover’s route on Mars. Because this procedure uses  
377 public datasets, it is applicable at will to both the already released Mastcam images available online  
378 and to the upcoming ones, as Curiosity rover keeps being driven on Mars. In addition, this  
379 procedure can be practical material for a pedagogic GIS project in Geosciences or Planetary  
380 Sciences, to handle Mars data both orbital and from the Curiosity rover. Perspectives include  
381 automation of this procedure, in order to automatically generate multiple Mastcam image  
382 viewsheds.

383

#### 384 **Acknowledgments**

385 We are grateful to the MSL engineers and scientists, and in particular the Mastcam Team, thanks  
386 to whom such awesome Mars datasets are acquired and made available.

387

#### 388 **References**

389 Arvidson, R. E., DeGrosse, P., Grotzinger, J. P., Heverly, M. C., Shechet, J., Moreland, S. J.,  
390 Newby, M. A., Stein, N., Steffy, A. C., Zhou, F., Zastrow, A. M., Vasavada, A. R., Fraeman,  
391 A. A., Stilly, E. K. 2017. “Relating geologic units and mobility system kinematics  
392 contributing to Curiosity wheel damage at Gale Crater, Mars.” *Journal of Terramechanics*.

393 Banham, S. G., S. Gupta, D. M. Rubin, J. A. Watkins, D. Y. Sumner, K. S. Edgett, J. P. Grotzinger,  
394 K. W. Lewis, L. A. Edgar, K. M. Stack-Morgan, R. Barnes, J. F. Bell, M. D. Day, R. C.  
395 Ewing, M. G. Lapotre, N. T. Stein, F. Rivera-Hernandez, A. R. Vasavada. 2018. “Ancient  
396 Martian Aeolian Processes and Palaeomorphology Reconstructed from the Stimson  
397 Formation on the Lower Slope of Aeolis Mons, Gale Crater, Mars.” *Sedimentology*.

398 Bell, J. F., A. Godber, S. McNair, M. A. Caplinger, J. N. Maki, M. T. Lemmon, J. Van Beek, M.  
399 C. Malin, D. Wellington, K. M. Kinch, M. B. Madsen, C. Hardgrove, M. A. Ravine, E. Jensen,  
400 D. Harker, R. B. Anderson, K. E. Herkenhoff, R. V. Morris, E. Cisneros, and R. G. Deen.  
401 2017. “The Mars Science Laboratory Curiosity Rover Mastcam Instruments: Preflight and  
402 in-Flight Calibration, Validation, and Data Archiving.” *Earth and Space Science*.

403 Bridges, N. T., R. Sullivan, C. E. Newman, S. Navarro, J. van Beek, R. C. Ewing, F. Ayoub, S.  
404 Silvestro, O. Gasnault, S. Le Mouélic, M. G. A. Lapotre, and W. Rapin. 2017. “Martian  
405 Aeolian Activity at the Bagnold Dunes, Gale Crater: The View from the Surface and Orbit.”

407 Calef III, F.J. and Parker, T., 2016, MSL Gale Merged Orthophoto Mosaic, Publisher: PDS Annex,  
408 U.S. Geological Survey, [http://bit.ly/MSL\\_Basemap](http://bit.ly/MSL_Basemap).

409 Dickson, J.L., Kerber, L.A., Fasett, C.I., and Ehlmann, B.L. 2018. "A Global, Blended CTX  
410 Mosaic of Mars with Vectorized Seam Mapping: A New Mosaicking Pipeline Using  
411 Principles of Non-Destructive Image Editing. 49<sup>th</sup> Lunar and Planetary Science Conference.  
412 Abstract 2480.

413 Ewing, R. C., M. G. A. Lapotre, K. W. Lewis, M. Day, N. Stein, D. M. Rubin, R. Sullivan, S.  
414 Banham, M. P. Lamb, N. T. Bridges, S. Gupta, and W. W. Fischer. 2017. "Sedimentary  
415 Processes of the Bagnold Dunes: Implications for the Eolian Rock Record of Mars." *Journal*  
416 *of Geophysical Research: Planets.*

417 Fraeman, A. A., B. L. Ehlmann, R. E. Arvidson, C. S. Edwards, J. P. Grotzinger, R. E. Milliken,  
418 D. P. Quinn, and M. S. Rice (2016), "The stratigraphy and evolution of lower Mount Sharp  
419 from spectral, morphological, and thermophysical orbital data sets," *J. Geophys. Res. Planets*,  
420 121,1713–1736, doi:10.1002/2016JE005095.

421 Grotzinger, J. P., S. Gupta, M. C. Malin, D. M. Rubin, J. Schieber, K. Siebach, D. Y. Sumner, K.  
422 M. Stack, A. R. Vasavada, R. E. Arvidson, F. Calef, L. Edgar, W. F. Fischer, J. A. Grant, J.  
423 Griffes, L. C. Kah, M. P. Lamb, K. W. Lewis, N. Mangold, M. E. Minitti, M. Palucis, M.  
424 Rice, R. M. E. Williams, R. A. Yingst, D. Blake, D. Blaney, P. Conrad, J. Crisp, W. E.  
425 Dietrich, G. Dromart, K. S. Edgett, R. C. Ewing, R. Gellert, J. A. Hurowitz, G. Kocurek, P.  
426 Mahaffy, M. J. McBride, S. M. McLennan, M. Mischna, D. Ming, R. Milliken, H. Newsom,  
427 D. Oehler, T. J. Parker, D. Vaniman, R. C. Wiens, and S. A. Wilson. 2015. "Deposition,  
428 Exhumation, and Paleoclimate of an Ancient Lake Deposit, Gale Crater, Mars." *Science*.

429 Le Deit, L., N. Mangold, O. Forni, A. Cousin, J. Lasue, S. Schröder, R.C. Wiens, D. Sumner, C.  
430 Fabre, K.M. Stack, R.B. Anderson, D. Blaney, S. Clegg, G. Dromart, M. Fisk, O. Gasnault,  
431 J.P. Grotzinger, S. Gupta, N. Lanza, S. Le Mouélic, A. Treiman. 2016. "The Potassic  
432 Sedimentary Rocks in Gale Crater, Mars, as Seen by ChemCam on Board Curiosity." *Journal*  
433 *of Geophysical Research: Planets.*

434 Lewis, K. W. and Turner, M.L. 2019. Geologic Structure of the Vera Rubin Ridge, Gale crater,  
435 Mars. 50<sup>th</sup> Lunar and Planetary Science Conference.

436 Malin, M. C., K. S. Edgett, E. Jensen, L. Lipkaman. 2013. "Mars Science Laboratory Project  
437 Software Interface Specification (SIS): Mast Camera (Mastcam), Mars Hand Lens Imager  
438 (MAHLI), and Mars Descent Imager (MARDI) Experimental Data Record (EDR) and  
439 Reduced Data Record (RDR) PDS Data Products."

440 Malin, M. C., M. A. Ravine, M. A. Caplinger, F. T. Ghaemi, J. A. Schaffner, J. N. Maki, J. F. Bell,  
441 J. F. Cameron, W. E. Dietrich, K. S. Edgett, L. J. Edwards, J. B. Garvin, B. Hallet, K. E.  
442 Herkenhoff, E. Heydari, L. C. Kah, M. T. Lemmon, M. E. Minitti, T. S. Olson, T. J. Parker,  
443 S. K. Rowland, J. Schieber, R. Sletten, R. J. Sullivan, D. Y. Sumner, R. Aileen Yingst, B. M.  
444 Duston, S. McNair, E. H. Jensen. 2017. "The Mars Science Laboratory (MSL) Mast Cameras  
445 and Descent Imager: Investigation and Instrument Descriptions." *Earth and Space Science*.

446 McEwen, A. S., and the HiRISE Science and Operations Team. 2018. "The future of  
447 MRO/HiRISE" *MEPAG Meeting 36, April 2018.*

- 448 [https://mepag.jpl.nasa.gov/meeting/abstracts/McEwen\\_HiRISEfuture.pdf](https://mepag.jpl.nasa.gov/meeting/abstracts/McEwen_HiRISEfuture.pdf).
- 449 McLennan, S. M., J. F. Bell Anderson, R B, F. Calef Bridges, J C, J. L. Campbell, B. C. Clark, S.  
450 Clegg, P. Conrad, A. Cousin, D. J. Des Marais, G. Dromart, M. D. Dyar, L. A. Edgar, B. L.  
451 Ehlmann, C. Fabre, O. Forni, O. Gasnault, R. Gellert, and S. Gordon. 2014. "Elemental  
452 Geochemistry of Sedimentary Rocks at Yellowknife Bay, Gale Crater, Mars." *Science*.
- 453 "MSL Coordinate Systems for Science Instruments." 2013.  
454 <https://an.rsl.wustl.edu/msl/mslbrowser/an3.aspx>.
- 455 Nachon, M., N. Mangold, O. Forni, L. C. Kah, A. Cousin, R. C. Wiens, R. Anderson, D. Blaney,  
456 J. G. Blank, F. Calef, S. M. Clegg, C. Fabre, M. R. Fisk, O. Gasnault, J. P. Grotzinger, R.  
457 Kronyak, N. L. Lanza, J. Lasue, L. Le Deit, S. Le Mouélic, S. Maurice, P. Y. Meslin, D. Z.  
458 Oehler, V. Payré, W. Rapin, S. Schröder, K. Stack, and D. Sumner. 2017. "Chemistry of  
459 Diagenetic Features Analyzed by ChemCam at Pahrump Hills, Gale Crater, Mars." *Icarus*.
- 460 Parker, T. J., M.C. Malin, F.J. Calef, R.G. Deen, H.E. Gengl, M.P. Golombek, J.R. Hall, O. Pariser,  
461 M. Powell, R.S. Sletten, and the MSL Science Team. 2013. "Localization and  
462 'contextualization' of Curiosity in Gale crater, and other landed mars missions". *44th Lunar  
463 and Planetary Science Conference, abstract 2534*.
- 464 Quinn, D.P. and Ehlmann, B.L. 2019. "A PCA-Based Framework for Determining Remotely  
465 Sensed Geological Surface Orientations and Their Statistical Quality." *Earth and Space  
466 Science*.
- 467 Stack, K. M., C. S. Edwards, J. P. Grotzinger, S. Gupta, D. Y. Sumner, F. J. Calef, L. A. Edgar,  
468 K. S. Edgett, A. A. Fraeman, S. R. Jacob, L. Le Deit, K. W. Lewis, M. S. Rice, D. Rubin, R.  
469 M. E. Williams, and K. H. Williford. 2016. "Comparing Orbiter and Rover Image-Based  
470 Mapping of an Ancient Sedimentary Environment, Aeolis Palus, Gale Crater, Mars." *Icarus*.
- 471 Stein N., Grotzinger J.P., Schieber J., N. Mangold, B. Hallet, H. Newsom, K.M. Stack, J.A. Berger,  
472 L. Thompson, Siebach K.L., Cousin A., Le Mouélic S., M. Minitti, D.Y. Sumner, C. Fedo,  
473 C.H. House, Gupta S., A.R. Vasavada, R. Gellert, Wiens. R. C., J. Fry, E. Dehouck. 2018.  
474 "Desiccation Cracks Provide Evidence of Lake Drying on Mars, Sutton Island Member,  
475 Murray Formation, Gale Crater." *Geology*.
- 476 Stein, N.T., Quinn, D.P., Grotzinger, J.P., Fedo, C., Ehlmann, B.L., Stack, K.M., Edgar, L.A.,  
477 Fraeman, A.A., and Deen, R. 2020. "Regional Structural Orientation of the Mt. Sharp Group  
478 Revealed by In-situ Dip Measurements and Stratigraphic Correlations on the Vera Rubin  
479 Ridge." *Journal of Geophysical Research: Planets*.
- 480 Sun, V. Z., K. M. Stack, L. C. Kah, L. Thompson, W. Fischer, A. J. Williams, S. S. Johnson, R.  
481 C. Wiens, R. E. Kronyak, M. Nachon, C. H. House, S. VanBommel. 2019. "Late-Stage  
482 Diagenetic Concretions in the Murray Formation, Gale Crater, Mars." *Icarus*.
- 483 Thompson, Lucy M. 2016. "Potassium-Rich Sandstones within the Gale Impact Crater, Mars: The  
484 APXS Perspective." *Journal of Geophysical Research: Planets*.
- 485 Weishu Gong. 2015. "Discussions on localization capabilities of MSL and MER rovers". *Annals  
486 of GIS*.
- 487 Wiens, R. C., D. M. Rubin, W. Goetz, A. G. Fairén, S. P. Schwenzer, J. R. Johnson, R. Milliken,

488 B. Clark, N. Mangold, K. M. Stack, D. Oehler, S. Rowland, M. Chan, D. Vaniman, S.  
489 Maurice, O. Gasnault, W. Rapin, S. Schroeder, S. Clegg, O. Forni, D. Blaney, A. Cousin, V.  
490 Payré, C. Fabre, M. Nachon, S. Le Mouelic, V. Sautter, S. Johnstone, F. Calef, A. R.  
491 Vasavada, and J. P. Grotzinger. 2017. “Centimeter to Decimeter Hollow Concretions and  
492 Voids in Gale Crater Sediments, Mars.” *Icarus*.